Synergistic effects of graphene–polyaniline counter electrode in dye-sensitised solar cells

Vorrada Loryuenyong[1,2], Sajjarinee Yaotrakool[1], Pratya Prathumted[1], Julaluck Lertsiri[1], Achanai Buasri[1,2]

[1]*Department of Materials Science and Engineering, Faculty of Engineering and Industrial Technology, Silpakorn University, Nakonpathom 73000, Thailand*
[2]*Center of Excellence on Petrochemical and Materials Technology, Chulalongkorn University, Bangkok 10330, Thailand*
E-mail: vorrada@gmail.com

Published in Micro & Nano Letters; Received on 8th September 2015; Revised on 21st November 2015; Accepted on 24th November 2015

This research studied the preparation of polyaniline/graphene hybrid material as a counter electrode in dye-sensitised solar cells by drop casting onto fluorine-doped tin oxide glass slides. Scanning electron microscope measurement revealed the rough surface of the hybrid films. The results have also shown that 1:2 ratio of PANI/graphene hybrid counter electrode provided a synergy that offered a comparable conversion efficiency to that of conventional Pt electrode.

1. Introduction: Dye-sensitised solar cells (DSSCs) are considered as one of the most attractive photovoltaic (PV) devices since their discovery by O'Regan and Grätzel in 1991 [1]. This is due to their high conversion efficiency, low cost, and simple fabrication. For the optimisation of manufacturing techniques, many researches have been developed into large-scale DSSCs production for practical and commercial applications [2]. Standard DSSCs consist of three primary components: a dye-sensitised TiO_2 photoanode, an iodide/triiodide (I^-/I_3^-) redox electrolyte, and a counter electrode [3]. The counter electrode is a conducting layer, which serves as an electrocatalyst for transferring and catalysing the reduction of triiodide (I_3^-) [4]. In general, a platinum (Pt)-coated conductive substrate is normally used due to its high conductivity and high catalytic activity for triiodide reduction. However, Pt is expensive, and the preparation of Pt counter electrode is both high energy-consuming and complicated. Therefore, many catalytic materials, such as graphene and conductive polymers, have been studied to replace Pt as counter electrodes for more cost-effective DSSCs.

Graphene is a new carbonaceous material with excellent chemical, optical, electrical, and physical properties. However, pure graphene is not effective on the reduction of triiodide in the iodide/triiodide redox reaction. This is because it is electrochemically inert and has poor electrolyte-interface compatibility and wettability. Therefore, graphene basal plane often restricts charge transfer at the graphene/electrolyte interface, although it has the high in-plane charge transfer. The DSSCs based on a transparent polyaniline (PANI)-graphene counter electrode has been reported as a good alternative to enhance the overall efficiency of the cells due to more photogenerated carriers, enhanced in-plane charge mobility, and excellent electrocatalytic activity for triiodide reduction [4–9]. For instance, Meng *et al.* [6] demonstrated an enhanced DSSC performance based on PANI-graphene complex/graphene oxide multilayers. In this work, an impressive power conversion efficiency of 7.88% has been achieved due to an increase in the reaction area of I^-/I_3^- redox species and the electron transfer between PANI and graphene. Therefore, it is envisaged that the nanocomposites of graphene and PANI should be able to provide improved performance for the use as the suitable counter electrode in DSSCs. In this Letter, we reported the replacement of Pt counter electrode in DSSCs by PANI/graphene hybrid films. The effects of PANI:graphene ratio on the conversion efficiency of DSSCs were also investigated.

2. Materials and method: The synthesis of PANI was performed via polymerisation method following the method reported in [3]. In a typical procedure, 25 mmol of aniline monomer (Applichem Panreac, Germany) was first dissolved in 50 ml 0.4 M HCl (Qrec, Germany) solution, and then another 50 ml 0.4 M HCl containing 8.3 mmol ammonium persulfate (Univar, Australia) was slowly dropped into the mixture. Polymerisation of aniline started after about 1 min, while the colour of the mixture changed into green. The mixture was kept at 4°C for 30 min. After that, it was filtered and washed with deionised water (DI). The obtained PANI salt was then dedoped with a diluted 0.4 M NaOH (Labscan, Ireland) solution for 15 min. The resultant PANI base was then filtered, washed with DI water several times, and dried at 60°C for 24 h.

For the preparation of PANI/graphene hybrid films, 0.1 g PANI was first dissolved in 25 ml N-methyl-2-pyrrolidone (NMP) (Sigma Aldrich, Germany) and stirred for a few minutes before graphene nanoplatelets (Grades 3, Graphene-Supermarket, USA) with various amounts was added into the solution. The suspension was then stirred and sonicated for another 30 min. The weight ratio of PANI to graphene was varied as 1:0 (pure PANI), 1:2, 1:4, 1:6 and 0:1 (pure graphene). PANI/graphene hybrid films were then prepared by a drop-coating method. Scotch tape was put on the conducting sides of a 1.5 cm × 2 cm fluorine-doped tin oxide (FTO) glass substrates (8 Ω/ð, Dyesol, Australia) to form 1 cm × 1 cm holes. The PANI/graphene hybrid dispersion was then dropped into the hole. The films were allowed to dry at room temperature for 3 days in a glove box before they were calcined at 200°C to remove the inorganic impurities and redoped with 1 M HCl for 4 h.

3. Characterisation: Fourier transform infrared (FTIR) spectra were recorded by using KBr as the background on a Bruker vertex 70. X-ray diffraction (XRD) patterns were obtained on a Shimadzu XRD-6100 by a powder XRD system equipped with a CuKα irradiation. The microstructure of the samples was investigated by scanning electron microscopy (SEM), and was obtained on a Camscan MX2000 operating at 15 kV. Cyclic voltammetry (CV) for the I^-/I_3^- system was conducted using Autolab PG STAT 101 at a scan rate of 0.1 V s^{-1}. A Pt wire and Ag/AgCl electrodes were used as auxiliary and reference electrodes, respectively, along with an electrolyte containing 0.01 M LiI, 1.0 mm I_2, and 0.1 M $LiClO_4$. UV-vis transmission spectra were obtained on a Shimadzu UV-1800. The PV performance of the cell was carried out by measuring the

current-voltage characteristic curves, using PXI source measure unit from National Instruments under an Abet Technologies Model 10500. The incident light intensity was controlled at 100 mW cm^{-2} (AM 1.5) solar simulator on an ABET 10500. The working electrode is commercial TiO_2 paste on FTO glass (Dyesol, Australia). The DSSCs were assembled by sandwiching the sensitised TiO_2 photoanode with PANI/graphene hybrid as a counter electrode, and the internal space was filled with electrolyte solution prepared by dissolving 0.05 M LiI (Sigma Aldrich, USA), 5 mmol I_2 (Carlo Erba, France) and 0.05 M 4-tertbutylpyridine (Sigma Aldrich, USA) in acetonitrile (Honeywell, USA) [10].

4. Results and discussion: The structures of PANI/graphene hybrids were characterised by the FTIR spectra, as shown in Fig. 1. Six different characteristic peaks are observed in the pure PANI spectrum (Fig. 1*a*) [11]. The bands at 1565 and 1495 cm^{-1} belong to the stretching of C=N and C=C in quinonoid and benzoquinone rings, respectively. The absorption bands at 1298 and 1245 cm^{-1} are attributed to the C-N stretching of benzoquinone ring. The characteristic peak at 1139 cm^{-1} is due to the quinonoid unit of doped PANI, while that at 802 cm^{-1} belongs to the out of plane bending of C-H in benzene ring. In the FTIR spectrum of graphene (0:1 ratio) (Fig. 1*e*), the peak around 1629 cm^{-1} is the characteristic absorption of the graphene skeleton-vibration, and the peaks around 1018 and 669 cm^{-1} are the characteristic peak of the C-O-C stretching. The FTIR curves of PANI/graphene hybrids (Figs. 1*b–d*) show the peak combination between PANI and graphene.

Fig. 2 shows the XRD patterns of PANI/graphene hybrid materials. For pure graphene (0:1 ratio), the diffraction peaks at $2\theta = 26.1°$ 37.8, 43.5°, 64.0° and 77.5° can be attributed to (002), (111), (200), (220) and (311) graphite-like structure, respectively. For pure PANI (1:0 ratio), a characteristic peak appears at 25.64°, which is accompanied by other two low intensity peaks at 20.38° and 15.22°, corresponding to (200), (020) and (011) crystal planes of PANI in its emeraldine salt form, respectively. The XRD pattern of the PANI/graphene hybrid materials exhibits four peaks similar to that of graphene. However, the peaks were shifted toward lower angle. This would be due to the intercalation of PANI between graphene layers.

The transparency of counter electrode is an important factor affecting incident light harvest from the film and the conversion efficiency of the DSSCs [12]. Fig. 3 compares the UV-Vis transmittance spectra of the six kinds of counter electrodes. All of the films on FTO glasses showed good transparency in the visible light range (400–800 nm), which could enhance the efficiency of the cells due to the light irradiation from the front and rear sides. However, an increase in graphene caused a decrease in light transmittance. According to experimental results, a large amount of graphene could cause the particle agglomeration on the film surfaces.

The morphologies of the samples were investigated by a SEM. Fig. 4 presents SEM images of PANI/graphene hybrid films. Both pure PANI (1:0 ratio) and graphene (0:1 ratio) films exhibited smooth morphologies. This would be because PANI could be dissolved, while graphene could be well-dispersed in NMP solution. The surfaces of hybrid films, on the other hand, possessed very high surface roughness, as can be seen from Figs. 4*b–d*. Graphene was not dissolved in NMP, and the incompatibility between PANI and graphene could cause the majority of graphene to agglomerate due to its van der Waals forces. This would lower the light transmittance of the hybrid films, as discussed in Fig. 3. Several reports, however, have shown that the counter electrode with high roughness would enhance its electrocatalytic activity for I^-/I_3^- redox reaction [13, 14].

CV was used to compare the electrocatalytic activity of Pt and PANI/graphene hybrid electrodes for I_3^-/I^- and I_2/I_3^- redox reactions in three electrodes at a scan rate of 100 mV s^{-1}, and the results are illustrated in Fig. 5. As seen from the figure, two pairs of redox peaks were observed in the CV curves of the PANI/graphene electrodes. The extreme left pair is associated with the redox reaction of I_3^-/I^- ($I_3^- + 2e^- \leftrightarrow 3I^-$), whereas the extreme right pair is related to the redox reaction of I_2/I_3^- ($3I_2 + 2e^- \leftrightarrow 2I_3^-$). The left redox pair in the CV curves determines the ability of the counter electrode towards the catalytic reduction of I_3^- to I^- in DSSCs. It is observed that the current density of this peak is higher for PANI/graphene electrode with ratio of 1:2, compared with that of Pt counter electrode, indicating the superior charge transfer of PANI/graphene electrode. However, Pt and graphene (0:1 ratio) have clearly cathodic reduction peaks, which could be attributed to the good electrocatalytic activity. Both the 1:4 and 1:6 ratio PANI/graphene electrode have lower current density than 1:2 ratio. This could be due to their low film qualities, which decrease charge transfer and conductivity.

The measurement of dark currents of DSSCs could provide useful information regarding to the back transfer process. Fig. 6 shows the dark current-voltage characteristics of the six kinds of counter electrodes with the applied voltage from 0 to 0.70 V. The onset of the dark current of PANI (1:0 ratio) occurred at high forward bias, while the 1:6 PANI/graphene hybrid film exhibited the ohmic behaviour leading to low V_{oc} and conversion efficiency.

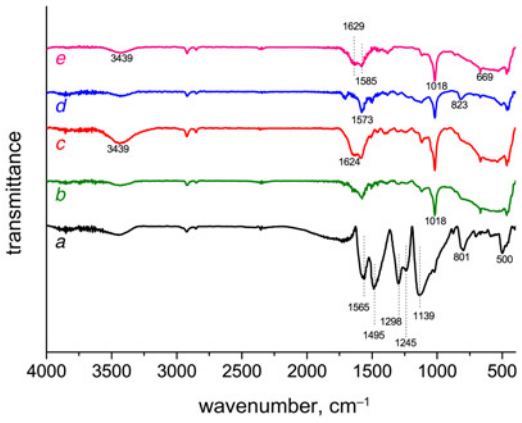

Fig. 1 *FTIR spectra of PANI/graphene hybrid materials*
a 1:0 (PANI)
b 1:2
c 1:4
d 1:6
e 0:1 (graphene)

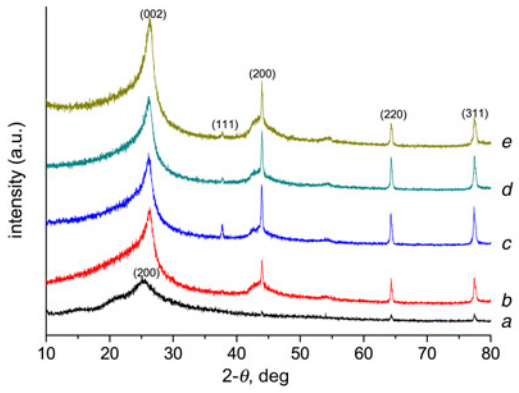

Fig. 2 *XRD spectra of PANI/graphene hybrid materials*
a 1:0 (PANI)
b 1:2
c 1:4
d 1:6
e 0:1 (graphene)

doi: 10.1049/mnl.2015.0363

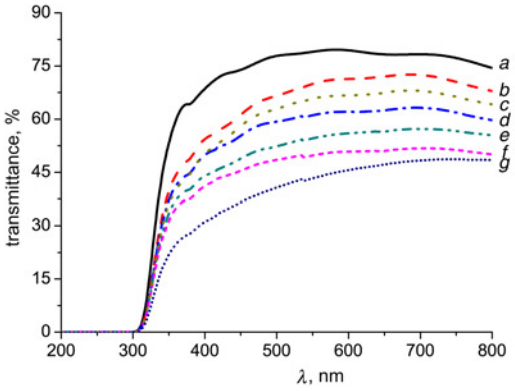

Fig. 3 *UV-Vis transmittance spectra of*
a FTO glass and counter electrodes from PANI/graphene hybrid film-coated FTO
b 1:0 (PANI)
c 1:0
d 1:2
e 1:4
f 1:6
g 0:1 (graphene)

This indicates that PANI could successfully reduce the reaction sites for the triiodide reduction by photoinjected electrons from TiO_2. Strikingly, the dark current curves of the 1:2 and 1:4 PANI/graphene hybrid films were shifted toward lower voltages and had lower dark currents than graphene and Pt counter electrodes. This indicated the suppression of charge recombination by the hybrid films with proper ratios of PANI/graphene.

To understand the feasible application of PANI/graphene hybrids in actual optoelectronic devices, the conversion efficiency of DSSCs was tested under one sun, AM 1.5 illumination. Photocurrent density-voltage characteristic curves of the DSSCs under illumination with different counter electrodes are shown in Fig. 6, and the corresponding PV parameters are summarised in Table 1. Compared with Pt counter electrode, the proper ratio (1:2) of PANI/graphene counter electrode had larger short circuit photocurrent density (J_{sc}). Such improvement could be attributed to the larger surface area and higher electrocatalytic ability of the PANI/graphene hybrid, resulting from the incorporation of highly conducting graphene. The higher value of open-circuit voltage (V_{oc}) and fill factor (FF) of Pt compared with the PANI/graphene electrode was due to its excellent electrical conductivity. Pt metal has lower charge transfer resistance, which is favourable for faster

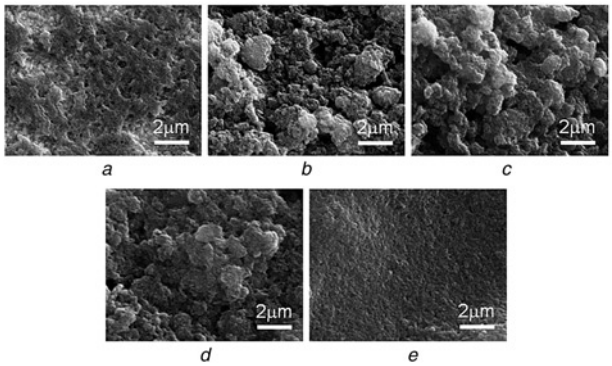

Fig. 4 *SEM images (5000x magnification) of PANI/graphene hybrid film-coated FTO*
a 1:0 (PANI)
b 1:2
c 1:4
d 1:6
e 0:1 (graphene)

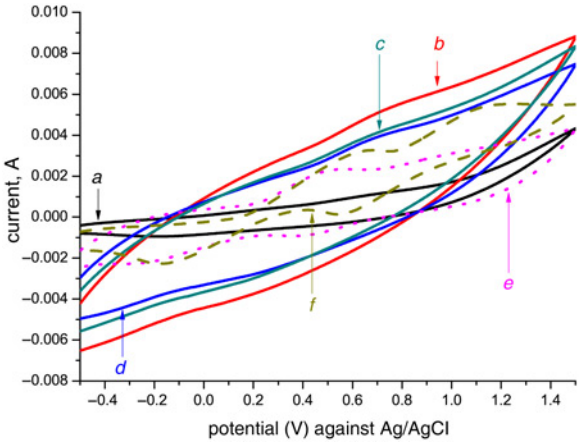

Fig. 5 *Cyclic voltammograms of PANI/graphene hybrid film-coated FTO*
a 1:0 (PANI)
b 1:2
c 1:4
d 1:6
e 0:1 (graphene)
f Pt counter electrodes

reduction of I_3^- ions. However, due to the high value of J_{sc} of the 1:2 PANI/graphene electrode, the overall efficiency value obtained was close to that of Pt electrode. As the contents of graphene in the

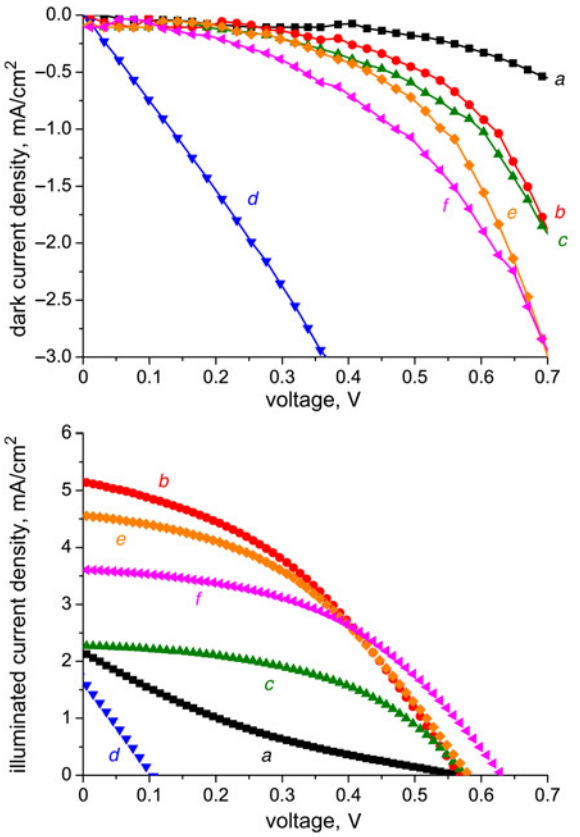

Fig. 6 *Dark current density-voltage characteristics of DSSC cells and current density-voltage characteristics of DSSC cells under one sun, AM 1.5 illumination with PANI/graphene hybrid film-coated FTO as counter electroders*
a 1:0 (PANI)
b 1:2
c 1:4
d 1:6
e 0:1 (graphene)
f Pt as counter electrodes

Table 1 PV parameters of DSSCs with various counter electrodes

Counter electrodes	V_{oc}, V	J_{sc}, mA cm^{-2}	FF	η, %
1:0 (PANI)	0.56	2.16	0.17	0.20
1:2	0.57	5.15	0.40	1.16
1:4	0.58	2.28	0.48	0.63
1:6	0.10	1.66	0.26	0.04
0:1 (graphene)	0.58	4.56	0.42	1.11
Pt	0.63	3.61	0.46	1.05

hybrid film increased (1:4 and 1:6 ratios), the conversion efficiency of DSSCs was decreased, which was consistent to CV measurement. PANI by itself was not an effective counter electrode due to its low electrical conductivity. In comparison with pure PANI and graphene, it could be wise to conclude that the obtained PANI/graphene composites exhibited better electrochemical performances and the conversion efficiency due to the synergistic effect between graphene and PANI, which was in consistent with previous works [2, 15].

5. Conclusion: PANI/graphene hybrid films with various ratios were successfully prepared by drop-casting the suspension onto FTO glass slides, which were then used as counter electrodes in DSSCs. The results showed that the hybrid films with PANI/graphene ratio of 1:2 could be used as a counter electrode in DSSCs to replace the conventional Pt counter electrode. This hybrid film showed higher electrocatalytic activity towards I_3^-/I^- reduction reaction as well as higher J_{sc} and higher FF value compared with pure PANI (1:0) and other hybrid films. This may be due to its efficient electron transport process and large active surface area. Thus, the PANI/graphene hybrid material has proven to be an effective alternative to the expensive Pt electrode for utilisation as next generation counter electrode in DSSCs.

6. Acknowledgments: This work was supported by Higher Education Research Promotion (HERP# 2558A11462006). The authors also wish to thank Department of Materials Science and Engineering, Faculty of Engineering and Industrial Technology, Silpakorn University, and Center of Excellence on Petrochemical and Materials Technology for supporting and encouraging this investigation.

7 References

[1] Bora C., Sarkar C., Mohan K.J., *ET AL.*: 'Polythiophene/graphene composite as a highly efficient platinum-free counter electrode in dye-sensitized solar cells', *Electrochim. Acta*, 2015, **157**, pp. 225–231
[2] Wan L., Wang B., Wang S., *ET AL.*: 'Water-soluble polyaniline/graphene prepared by in situ polymerization in graphene dispersions and use as counter-electrode materials for dye-sensitized solar cells', *React. Funct. Polym.*, 2014, **79**, pp. 47–53
[3] Tai Q., Chen B., Guo F., *ET AL.*: 'In situ prepared transparent polyaniline electrode and its application in bifacial dye-sensitized solar cells', *ACS Nano*, 2011, **5**, (5), pp. 3795–3799
[4] Wang G., Zhuo S., Xing W.: 'Graphene/polyaniline nanocomposite as counter electrode of dye-sensitized solar cells', *Mater. Lett.*, 2012, **69**, pp. 27–29
[5] Liu C.-Y., Huang K.-C., Chung P.-H., *ET AL.*: 'Graphene-modified polyaniline as the catalyst material for the counter electrode of a dye-sensitized solar cell', *J. Power Sources*, 2012, **217**, pp. 152–157
[6] Meng Y., Wang K., Zhang Y., *ET AL.*: 'Hierarchical porous graphene/polyaniline composite film with superior rate performance for flexible supercapacitors', *Mater.*, 2013, **25**, (48), pp. 6985–6990
[7] Wang M., Tang Q., Xu P., *ET AL.*: 'Counter electrodes from polyaniline-graphene complex/graphene oxide multilayers for dye-sensitized solar cells', *Electrochim. Acta*, 2014, **137**, pp. 175–182
[8] Wang G., Xing W., Zhuo S.: 'The production of polyaniline/graphene hybrids for use as a counter electrode in dye-sensitized solar cells', *Electrochim. Acta*, 2012, **66**, pp. 151–157
[9] Wang M., Tang Q., Chen H., *ET AL.*: 'Counter electrodes from polyaniline–carbon nanotubecomplex/graphene oxide multilayers for dye-sensitizedsolar cell application', *Electrochim. Acta*, 2014, **125**, pp. 510–515
[10] Al-bahrani M.R., Xu X., Ahmada W., *ET AL.*: 'Highly efficient dye-sensitized solar cell with GNS/MWCNT/PANI as a counter electrode', *Mater. Res. Bull.*, 2014, **59**, pp. 272–277
[11] Trchová M., Stejskal J.: 'Polyaniline: The infrared spectroscopy of conducting polymer nanotubes (IUPAC Technical Report)', *Pure Appl. Chem.*, 2011, **83**, (10), pp. 1803–1817
[12] Alvi F., Ram M.K., Basnayaka P.A., *ET AL.*: 'Graphene–polyethylenedioxythiophene conducting polymer nanocomposite based supercapacitor', *Electrochim. Acta*, 2011, **56**, (25), pp. 9406–9412
[13] Chen J.G., Wei H.Y., Ho K.C.: 'Using modified poly(3,4-ethylene dioxythiophene): Poly(styrene sulfonate) film as a counter electrode in dye-sensitized solar cells', *Sol. Energy Mater. Sol. Cells*, 2007, **91**, pp. 1472–1477
[14] Yen M.-Y., Hsieh C.-K., Teng C.-C., *ET AL.*: 'Metal-free, nitrogen-doped graphene used as a novel catalyst for dye-sensitized solar cell counter electrodes', *RSC Adv.*, 2012, **2**, pp. 2725–2728
[15] Li Y., Peng H., Li G., *ET AL.*: 'Synthesis and electrochemical performance of sandwich-like polyaniline/graphene composite nanosheets', *Eur. Polym. J.*, 2012, **48**, pp. 1406–1412

doi: 10.1049/mnl.2015.0363